Trifluoromethyl Hypobromite, CF_3OBr[†]

Rolf Minkwitz,* Raimund Bröchler, and Andreas Kornath

Anorganische Chemie, Fachbereich Chemie, Universität Dortmund, 44221 Dortmund, Germany

Ralf Ludwig and Frank Rittner

Physikalische Chemie, Fachbereich Chemie, Universität Dortmund, 44221 Dortmund, Germany

Received September 11, 1996[⊗]

The synthesis and isolation of the hypobromite CF_3OBr is reported. CF_3OBr is formed besides $Me_4N^+BrF_2^-$ by the reaction of CF_3OCl and $Me_4N^+Br_3^-$ via an addition−elimination mechanism. The initially formed solid, $[2CF_3OBr{\cdot}Me_4N^+BrF_2^-]$, was characterized by ^{13}C and ^{19}F NMR, Raman, IR, and mass spectra. The hypobromite was separated from the solid by high-vacuum condensation onto a cold surface and characterized by matrix isolation multichannel Raman spectroscopy. An ab initio calculation was performed, and a force field and the torsional barrier of CF_3OBr were calculated. The calculation predicts an eclipsed conformation with a rotional barrier of 3.4 kcal/mol. The photolytic decomposition of CF_3OBr in the solid state and in an argon matrix was investigated.

Introduction

The first results on the synthesis and isolation of organofluorine hypohalites appeared in 1948, when trifluoromethyl hypofluorite CF_3OF was identified.[1] The hypochlorite CF_3OCl was described 20 years later for the first time.[2,3] An attempt to prepare the unknown hypobromite CF_3OBr was carried out by Lorenzen-Schmidt et al.[4,5] in 1994 and 1995. It was formed in a matrix cage during the course of the reaction of $^{18}O_3$ with CF_3Br. Evidence for the existence of this molecule is based only on three observed bands for the CF_3 group.

The existing methods for the preparation of organofluorine hypohalites can be arbitrarily divided into catalytic and noncatalytic. The most important method for the preparation of CF_3OX (X = F, Cl) is the catalyzed action of F_2 or ClF on carbonyl difluoride. The CsF-catalyzed reaction of bromine fluoride with carbonyl difluoride seems not to be successful because the reaction temperature is above the decomposition temperature of bromine fluoride. Our attempts to prepare CF_3OBr from BrCl and CF_3OCl gave only low yields of impure product. During our investigation of the synthetic potential[6−8] of CF_3OCl, we found an unusual way to prepare the hypobromite in high purity.

The CF_3OBr seems to play a role as an intermediate decomposition product in the course of the ozone layer depletion by halones such as CF_3Br, whose emission is on the order of 1820 tons/year.[9]

Experimental Section

All synthetic work and sample handling were performed by employing standard Schlenk techniques and a standard glass vacuum line. The glass vacuum line and the reaction vessels were treated with CF_3OCl prior to use. Nonvolatile materials were handled under dry nitrogen. CF_3OCl was prepared in a stainless steel vessel, from F_2CO and ClF using CsF as catalyst.[10,11]

Infrared spectra were recorded on a Bruker ifs 113v spectrophotometer. Spectra of dry powders were obtained in a low-temperature cell between CsI plates. The Raman spectra were recorded on a Jobin Yvon T64000 spectrometer using an Ar^+ laser (514.5 nm) from Spectra Physics. The spectra of $[2CF_3OBr{\cdot}Me_4N^+BrF_2^-]$ were recorded in a glass tube cooled with liquid nitrogen. The ^{19}F (262 MHz) and ^{13}C (75.432 MHz) NMR spectra were obtained in CH_3CN on a Bruker DPX 300 with $CFCl_3$ used as internal reference. The mass spectra were recorded on a Finnigan MAT CH-5.

Preparation of $[2CF_3OBr{\cdot}Me_4N^+BrF_2^-]$. CF_3OCl (964 mg 8 mmol) was condensed into a dry 50 mL glass vessel onto 313 mg (1 mmol) of $Me_4N^+Br_3^-$. The reaction mixture was allowed to warm slowly to −70 °C and kept at this temperature for 3 days. After removal of the volatile materials at −90 °C under vacuum, a colorless, extremely moisture-sensitive solid was obtained. It is stable below −50 °C. The salt is soluble in dry CH_3CN, but slowly decomposes at −35 °C to $Me_4N^+BrF_4^-$, F_2CO, BrF_3, and Br_2. Therefore, the NMR spectra show, besides the product signals, those of the decomposition products. Spectral data are as follows. ^{19}F NMR (in CH_3CN): ϕ −55.0 (s) (CF_3OBr); ϕ −41.5 (s) (BrF_2^-); ϕ −35.7 (s) (BrF_4^-); ϕ −20.2 (s) (F_2CO); ϕ −15.8 (s) (BrF_3). ^{13}C NMR (in CH_3CN): δ 133.5 (t), J_{CF} 308 Hz (F_2CO); δ 118.9 (q), J_{CF} 261 Hz (CF_3OBr); δ 54.3 (t), J_{CH} 4 Hz (Me_4N^+). MS (70 eV, −40 °C) (*m*/*z* (fragment), relative intensty): 174/176/178 (Br_2O^+), 16/30/15; 164/166 (CF_3OBr^+), 73/72; 158/160/162 (Br_2^+), 44/64/44; 145/147 (F_2COBr), 6/7; 98/100 (BrF^+), 31/29; 95/97 (BrO^+), 20/19; 79/81 (Br^+), 75/74; 69 (CF_3^+), 72; 66 (F_2CO), 88; 50 (CF_2^+), 19; 47 (COF^+), 100. Infrared (solid, ∼ −70 °C), cm^{-1}: 3050 w, 1487 vs, 1419 s, 1312 vs, 1244 vs (br), 1118 s (br), 949 s, 908 m, 892 m, 713 s, 708 sh, 654 s, 617 m, 511 s, 449 s, 316 vs, 302 sh, 213 s. Raman (solid, −78 °C), cm^{-1}: 3053 m, 2996 s, 2971 m, 2939 m, 2910 w, 2880 vw, 2833 m, 1491 vw, 1461 m, 1428 m, 1325 w, 1305 w, 1293 w, 1238 sh, 1222 m, 1174 w, 1113 w, 955

[†] Raman Matrix Spectroscopy. 2. Part 1: Kornath, A. *J. Raman Spectrosc.* **1997**, *28*, 9.

[⊗] Abstract published in *Advance ACS Abstracts,* April 15, 1997.

(1) Kellog, K. B.; Cady, G. H. *J. Am. Chem. Soc.* **1948**, *70*, 3986.
(2) Gould, D. E.; Anderson, L. R.; Young, D. E.; Fox, W. B. *J. Chem. Soc., Chem. Commun.* **1968**, 1564.
(3) Schack, C. J.; Maya, W. *J. Am. Chem. Soc.* **1969**, *91*, 2902.
(4) Lorenzen-Schmidt, H.; Weller, R.; Schrems, O. *Ber. Bunsen-Ges. Phys. Chem.* **1994**, *98*,1622.
(5) Lorenzen-Schmidt, H.; Weller, R.; Schrems, O. *J. Mol. Struct.* **1995**, *349*, 333.
(6) Minkwitz, R.; Bröchler, R.; Preut, H. *Z. Anorg. Allg. Chem.* **1995**, *621*, 1247.
(7) Minkwitz, R.; Bröchler, R.; Schütze, M. *Z. Anorg. Allg. Chem.* **1995**, *621*, 1727.
(8) Minkwitz, R.; Bröchler, R.; Berkei, M. *Z. Anorg. Allg. Chem.* **1996**, *622*, 1749.
(9) Krüger, B. C.; Fabian, P. *Ber. Bunsen-Ges. Phys. Chem.* **1986**, *90*, 1062.
(10) Gould, D. E.; Anderson, L. R.; Young, D.; Fox, W. B. *J. Am. Chem. Soc.* **1969**, *91*, 1310.
(11) Schack, C. J.; Maya, W. *J. Am. Chem. Soc.* **1969**, *91*, 2902.

S0020-1669(96)01113-5 CCC: $14.00

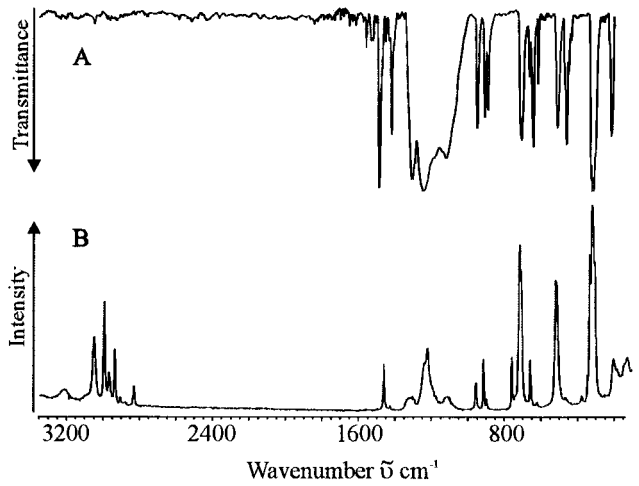

Figure 1. Vibrational spectra of $[2CF_3OBr{\cdot}NMe_4BrF_2]$: trace A, IR spectrum of the solid on a CsI plate at −90 °C; trace B, Raman spectrum of the solid at −78 °C.

m, 914 m, 896 w, 758 m, 716 vs, 656 m, 619 w, 516 s, 459 w, 372 w, 342 m, 329 vs, 316 vs, 303 vs, 199 m, 122 m.

Isolation of CF_3OBr. The apparatus previously described for multichannel Raman matrix spectroscopy[12] was used for the isolation of solid CF_3OBr. A dry 35 mL glass vessel containing 150 mg of $[2CF_3OBr{\cdot}Me_4N^+BrF_2^-]$ was connected to the condensation tube of the apparatus. The glass vessel was slowly warmed from −70 to −50 °C, and the volatile CF_3OBr was condensed at a pressure of less than 5×10^{-6} hPa (mbar) onto the cold surface (−258 °C). Experiments to obtain an argon matrix layer by passing the rare gas over the decomposing solid were unsuccessful. Therefore, the evolved CF_3OBr was mixed with argon in front of the cold surface. The pressure increased during the condensation up to 2×10^{-5} hPa (mbar).

Results and Discussion

Formation of $[2CF_3OBr{\cdot}Me_4N^+BrF_2^-]$. The tribromide $NMe_4^+Br_3^-$ reacts at −70 °C with an excess of CF_3OCl with the formation of the solid $[2CF_3OBr{\cdot}Me_4N^+BrF_2^-]$, Cl_2, and F_2CO according to reaction I.

$$4CF_3OCl + Me_4N^+Br_3^- \xrightarrow[CF_3OCl]{-70\ ^\circ C} \underset{\mathbf{I}}{[2CF_3OBr{\cdot}Me_4N^+BrF_2^-]} + Cl_2 + 2F_2CO \quad (I)$$

The reaction products were characterized by vibrational spectroscopy. The Raman and IR spectra of **I** are shown in Figure 1 and are discussed later. The colorless $[2CF_3OBr{\cdot}Me_4N^+BrF_2^-]$ is soluble in dry acetonitrile with slow decomposition at −35 °C. Therefore, the ^{19}F NMR spectrum shows, besides the signals of CF_3OBr at −55 ppm and of BrF_2^- at −41.5 ppm, the signals for the decomposition products BrF_4^- at −35.7 ppm (−37 ppm),[13] F_2CO at −20.2 ppm, and BrF_3 at −15.8 ppm (−16.3 ppm).[14] Attempts to obtain single crystals failed because of the instability in solution.

The unusual reaction (I) proceeds in several steps, probably via an addition−elimination mechanism proposed in Scheme 1. First the positively polarized chlorine of CF_3OCl may attack the tribromide, forming CF_3OBr and $BrCl_2^-$, which may then undergo further reaction with formation of BrF_2^-, Cl_2, and F_2CO.

Decomposition of $[2CF_3OBr{\cdot}Me_4N^+BrF_2^-]$. The first indication for CF_3OBr was obtained from the MS spectra of

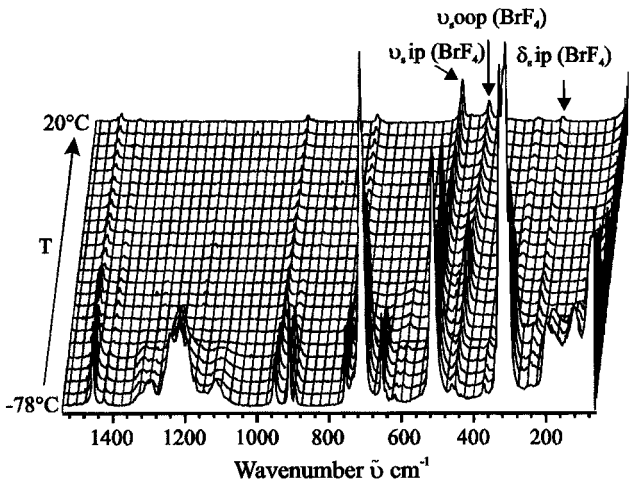

Figure 2. Raman spectra of $[2CF_3OBr{\cdot}NMe_4BrF_2]$ during the removal of CF_3OBr in the temperature range from −70 °C to room temperature.

Scheme 1. Proposed Reaction Route for the Formation of $[2F_3OBr{\cdot}NMe_4BrF_2]$

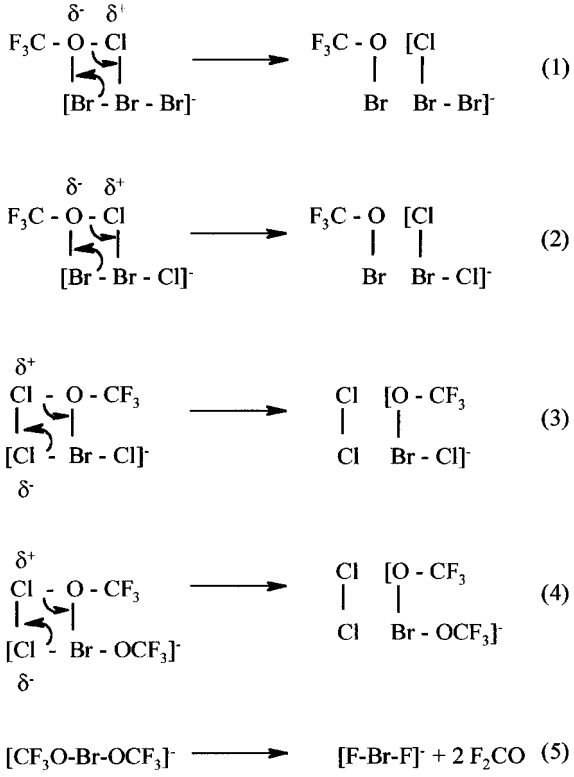

compound **I**. The MS spectra show the molecular peak of CF_3OBr and its fragments. More detailed information was obtained by recording Raman spectra during the decomposition of **I**. Figure 2 shows the vacuum thermolysis of **I** in the temperature range between −78 °C and room temperature.

The spectra of $[2CF_3OBr{\cdot}Me_4N^+BrF_2^-]$ before decomposition in Figure 1 show the bands of CF_3OBr, as discussed later, accompanied by the typical bands of the tetramethylammonium cation.[13] The Raman-active symmetric Br−F stretching mode of BrF_2^- coincides with the antisymmetric CF_3 deformation of CF_3OBr at 516 cm^{-1}. During the decomposition (Figure 2) under vacuum, the CF_3OBr is removed completely while the residual $Me_4N^+BrF_2^-$ decomposes further to give $Me_4N^+BrF_4^-$ and $Me_4N^+Br^-$(reaction II). Therefore, the line at 516 cm^{-1} is replaced by the three Raman-active lines of BrF_4^- during the decomposition. The final spectrum in Figure 2 consists of pure

(12) Kornath, A.; Köper, I. *J. Raman Spectrosc.*, in press.
(13) Wilson, W. W.; Christe, K. O. *Inorg. Chem.* **1989**, *28*, 4172
(14) Breuer, W.; Frohn, H. J. *J. Fluorine Chem.* **1987**, *34*, 443.

Table 1. Raman Data[a] for CF_3OBr Compared to Those for CF_3OF and CF_3OCl

CF_3OF[b]		CF_3OCl[b]		CF_3OBr		
liquid	Ar matrix	liquid	Ar matrix	solid	Ar matrix	assignt
1310 (1)	1288 (5)	1275 (3)	1269 (17)	1263 (6)	1251 (3)	$\nu_{as}(CF_3)$, A′
	1250 (7)		1221 (8)	1176 (16)	1170 (6)	$\nu_{as}(CF_3)$, A″
1205 (3)	1211 (14)	1190 (2)	1200 (3)	1140 (6)		$\nu_s(CF_3)$ A′
				1103 (5)		
				986 (7)	981 (14)	(661 + 332)
946 (16)	945(54)	917 (26)	920 (28)	914 (36)	914 (35)	ν(CO), A′
882 (100)	883(100)	781 (100)	783 (100)	732 (100)	734 (66)	ν(OX), A′
				727 (89)	725 (88)	
868 (8)	871 (7)					2δ(COF), A′
			776 (24)			$\nu(O^{37}Cl)$, A′
679 (12)	678 (24)	666 (15)	663 (30)	661 (21)	659 (27)	$\delta_s(CF_3)$, A′
609 (3)	606 (9)	611 (3)	609 (15)	617 (4)	615 (6)	$\delta_{as}(CF_3)$, A″
587 (5)	582 (9)	561 (14)	558 (28)	527 (85)	527 (90)	$\delta_{as}(CF_3)$, A′
		548 (12)	547 (9)			$CF_3OCl\cdots Cl_2$
			539 (10)			
		430 (1)		436 (2)	438 (4)	$\rho(CF_3)$, A″
436 (10)	433(34)	397 (41)	398 (62)	346 (66)	345 (89)	δ(COX), A′
				340 (83)	337 (100)	
				332 (92)	320 (sh)	
259 (3)	256 (16)	220 (4)	239 (5)	194 (20)	191 (23)	$\rho(CF_3)$, A′
285 (sh)		235 (sh)				$2\tau(CF_3)$, A′
144 (5)		122 (6)		131 (6)	128 (3)	$\tau(CF_3)$, A″

[a] Frequencies in cm^{-1}. [b] Data from ref 15.

$$2[2CF_3OBr\cdot Me_4N^+BrF_2^-] \xrightarrow{-50\ ^\circ C} 4CF_3OBr + Me_4N^+BrF_4^- + Me_4N^+Br^- \quad (II)$$

$Me_4N^+BrF_4^-$ (ν_s(in phase)(Br−F) 520 cm^{-1}; ν_s(out of phase)-(Br−F) 447 cm^{-1}; δ_s(in plane) 240 cm^{-1}).[13]

Raman Spectra of CF_3OBr. The Raman spectra of solid and matrix-isolated CF_3OBr are shown in Figure 3. The vibrations of CF_3OBr were assigned by comparison with those of the known hypohalites CF_3OF[15] and CF_3OCl[15] and the ab initio calculation, which gave a structure of symmetry C_s. The observed and calculated frequencies of CF_3OBr are summarized in Table 3.

The weak lines at 1263, 1176, and 1140 cm^{-1} are assigned to the CF stretching modes of the CF_3O group and are comparable to those of CF_3OF,[15] 1310 and 1205 cm^{-1}, and of CF_3OCl,[15] 1275 and 1190 cm^{-1}. The line at 914 cm^{-1} belongs to the CO stretching mode, which is observed at 946 cm^{-1} for CF_3OF and 917 cm^{-1} for CF_3OCl. A typical intense line for hypohalites is the oxygen−halogen stretching mode. It occurs for the two known hypobromites at 761 cm^{-1} (O_2NOBr)[16] and 659 cm^{-1} ($F(O_2)SOBr$),[17] respectively. The OBr stretching mode of CF_3OBr is observed at 732/727 cm^{-1}.

The deformation modes occur in the region below 700 cm^{-1}. The three lines at 661, 617, and 527 cm^{-1} are assigned to CF_3 deformation modes by analogy with the assigned absorptions for CF_3OF, 679, 609, and 587 cm^{-1}, and CF_3OCl, 666, 611, and 561 cm^{-1}. Comparing the CF_3 deformation modes of the hypohalites, one can see an inversion of the intensities. For CF_3OF[15] the relative intensities are (12), (3), (5), for CF_3OCl[15] (30), (15), (28), and for CF_3OBr (21), (4), (85). The triply split line at 346/340/332 belongs to the COBr deformation mode. This COX deformation appears at 436 cm^{-1} for CF_3OF and 397 cm^{-1} for CF_3OCl. The rocking deformation mode of CF_3 is expected to occur in the frequency region below 200 cm^{-1} and is assigned to the 194 cm^{-1} band. The line at 131 cm^{-1} is assigned to the torsional mode by analogy to CF_3OF (144 cm^{-1}) and CF_3OCl (122 cm^{-1}). The ab initio calculation gave a lower value of 89 cm^{-1} for the gas phase. This discrepancy is in accord with the torsional modes of CF_3OF[18] and CF_3OCl,[18] which have already been described by Hammaker et al.

Table 2. Experimental and Calculated (Eclipsed Conformation) Vibrational Data[a] for CF_3OBr

calcd freq		obsd Raman freq		
HF 6-311G*	MP 2 6-31G*	solid	Ar matrix	assignt
1314	1256	1263	1251	$\nu_{as}(CF_3)$, A′
1267	1208	1176	1170	$\nu_{as}(CF_3)$, A″
1266	1191	1140		$\nu_s(CF_3)$, A′
926	872	914	914	ν(CO), A′
742	692	732/727	734/725	ν(OX), A′
650	619	661	659	$\delta_s(CF_3)$, A′
603	575	617	615	$\delta_{as}(CF_3)$, A″
521	499	527	527	$\delta_{as}(CF_3)$, A′
425	402	436	438	$\rho(CF_3)$, A″
341	326	346/340/332	345/337/320	δ(COX), A′
173	172	194	191	$\rho(CF_3)$, A″
93	100	130	128	$\tau(CF_3)$, A″

[a] Frequencies in cm^{-1}.

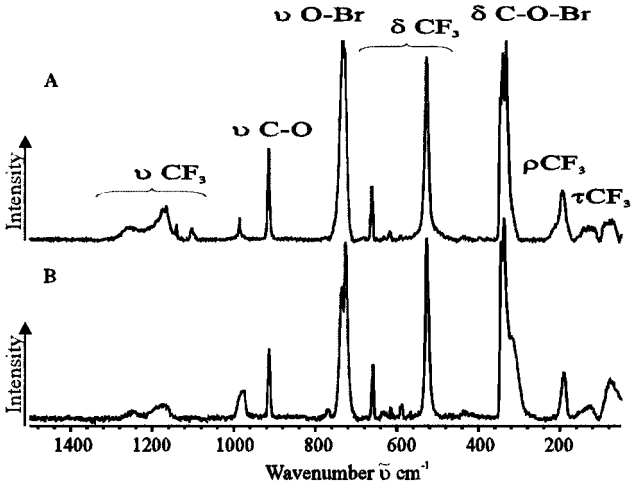

Figure 3. Raman spectra of CF_3OBr at 15 K: trace A, solid CF_3OBr; trace B, CF_3OBr in an argon matrix (M:R = 1:250). Experimental conditions: laser, 250 mW; slit, 100 μm; integration time, 300 s.

(15) Kuo, J. C.; DesMarteau, D. D.; Fateley, W. G.; Hammaker, R. M.; Marsden, C. J.; Witt, J. D. *J. Raman Spectrosc.* **1980**, *9*, 230.
(16) Wilson, W. W.; Christe, K. O. *Inorg. Chem.* **1987**, *26*, 1573.
(17) Aubke, F.; DesMarteau, D. D. *Fluorine Chem. Rev.* **1977**, *8*, 74.

Table 3. Calculated Frequencies[a] for the Eclipsed and Staggered Conformations of CF_3OBr

calcd freq[a]				
eclipsed conformn		staggered conformn		
HF 6-311G*	MP2 6-31G*	HF 6-311G*	MP2 6-31G*	assignt
1314	1256	1300	1248	$\nu_{as}(CF_3)$, A′
1267	1208	1279	1220	$\nu_{as}(CF_3)$, A″
1266	1191	1255	1174	$\nu_{s}(CF_3)$, A′
926	872	936	880	ν(CO), A′
742	692	738	693	ν(OX), A′
650	619	647	618	$\delta_{s}(CF_3)$, A′
603	575	596	568	$\delta_{as}(CF_3)$, A″
521	499	510	487	$\delta_{as}(CF_3)$, A′
425	402	407	377	$\rho(CF_3)$, A″
341	326	337	319	δ(COX), A′
173	172	202	205	$\rho(CF_3)$, A′
93	100	−82	−89	$\tau(CF_3)$, A″

[a] Frequencies in cm^{-1}.

Besides the 12 fundamental vibrations, a weak line at 986 cm^{-1} was observed which we attribute to a combination of the CF_3 and the COBr deformation modes (332 + 661 = 993).

During the Raman experiments, it was found that CF_3OBr partially decomposes by irradiation with the laser beam (514.5 nm). The matrix-isolated CF_3OBr was stable for a long period, and decomposition was only measured by an incident laser power of more than 250 mW. The photolysis of CF_3OBr produces mainly bromine and various still-unidentified organofluorine compounds. In contrast to the thermal decomposition, formation of F_2CO was not observed.

Ab Initio Calculation. The restricted Hartree−Fock calculations were performed with the Gaussian-94 program[19] using Gaussian-type basis functions. The energy minima with respect to nuclear coordinates were obtained by the simultaneous relaxation of all the geometric parameters using the gradient method of Pulay.[20] The calculated structural parameters were determined with RHF/6-31G* and RHF/6-311G* calculations, along with electron correlation at the MP2/6-31G* level.[21]

For the C_s constrained symmetric structure, the fluoride atom of the trifluoromethyl group can be positioned in two different orientations with respect to the O−Br bond. The relative stabilities of these conformations can be judged by investigating the potential surface. Therefore the torsional potential function was estimated at the RHF/6-311G* level of theory by optimizing the geometry with fixed values of the torsional angle F−C−O−Br at 10° increments (from 0 to 180°). All other structural parameters were allowed to relax in the computation. The assigned torsional frequency for the solid phase and the calculated barrier for the vapor state are shown in Table 5 and compared to those of several CF_3 rotors in other C_s molecules.[18] Selected calculated geometry parameters of CF_3OBr (eclipsed conformation) compared to those for CF_3OF[22] and CF_3OCl[23] are given in Table 4.

Table 4. Selected Calculated Geometric Parameters[a] for CF_3OBr (Eclipsed Conformation) Compared to Those for CF_3OF and CF_3OCl

			CF_3OBr	
	CF_3OF[b]	CF_3OCl[c]	HF 6-31 G*	MP2 6-31G*
r(CF)	131.9(3)	132.5(3)	131.0	133.8
r(CO)	139.5(6)	136.5(7)	135.1	137.7
r(OX)	142.1(6)	167.9(3)	180.6	186.9
∠(FCF)	109.4(10)	109.2(7)	108.2	108.7
∠(COX)	104.9(6)	112.9(5)	120.5	111.9

[a] Bond distances in pm and angles in degrees. [b] Bond distances from ref 22. [c] Bond distances from ref 23.

Table 5. Assigned Torsional Frequencies for the Solid Phase and Calculated Barriers for the Vapor State of CF_3OBr Compared to Those for Several CF_3 Rotors[a] in Other C_s Molecules

			CF_3OBr			
	CF_3-OF[b]	CF_3-OCl[b]	Raman, solid	RHF 6-311G*	CF_3-OOF[b]	CF_3-OOCl[b]
ν_t (cm^{-1})	144	122	131	93	78	80
V (kcal mol^{-1})	4.64	4.6		3.4	2.9	3.7

[a] Frequencies for the liquids and calculated barriers for the vapor state. [b] Data from ref 18.

The calculated frequencies for the energetically favored staggered structure as well as for the eclipsed conformation are shown in Table 3. As expected, no imaginary frequencies were found for the eclipsed conformation, whereas for the staggered conformation one imaginary vibrational frequency was found, indicative of a transition state.

The calculated frequencies seem to be generally 10% too high at the Hartree−Fock level[24,25] and decrease to 5% when electron correlations are taken into account.[26]

Acknowledgment. This work was supported by the Fonds der chemischen Industrie and the Deutsche Forschungsgemeinschaft.

IC961113F

(18) Hammaker, R. M.; Fateley, W. G.; Manocha, A. S.; DesMarteau, D. D.; Streusand, B. J.; Durig, J. R. *J. Raman Spectrosc.* **1980**, *9*, 181.
(19) Frisch, M. J.; Trucks, G. W.; Schlegel, H. B.; Gill, P. M. W.; Johnson, B. G.; Robb, M. A.; Cheeseman, J. R.; Keith, T. A.; Peterson, G. A.; Montgomery, J. A.; Raghavachari, K.; Laham, M. A.; Zakrzewski, V. G.; Ortiz, J. V.; Foresman, J. B.; Ciolowski, J.; Stefanov, B.; Nanayakkara, A.; Challacombe, M.; Peng, C. Y.; Ayala, P. Y.; Chen, W.; Wong, M. W.; Andres, J. L.; Replogle, E. S.; Gomperts, R.; Martin, R. L.; Fox, D. J.; Binkley, J. S.; Defrees, D. J.; Baker, J.; Steward, J. J. P.; Head-Gordon, M.; Gonzales, C.; Pople, J. A. *Gaussian 94*, revision A.1; Gaussian, Inc.: Pittsburgh, PA, 1995.
(20) Pulay, P. *J. Comput. Chem.* **1982**, *3*, 556.
(21) For an authoritative description of the ab initio methods and basis sets employed here, see: Hehre, W. G.; Radom, L.; Schleyer, P. v. R.; Pople, J. A. *Ab Initio Molecular Orbital Theory*; Wiley: New York, 1986.
(22) Diodati, F. P.; Bartell, L. S. *J. Mol. Struct.* **1971**, *8*, 395.
(23) Oberhammer, H.; Mahmood, T.; Shreeve, J. *J. Mol. Struct.* **1984**, *117*, 311.
(24) Pulay, P.; Forgarasi, G.; Pang, F.; Boggs, J. E. *J. Am. Chem. Soc.* **1979**, *101*, 2550.
(25) Pople, J. A.; Schlegel, H. B.; Krishnan, R.; Frees, D. J.; Binkley, J. S.; Frisch, M. J.; Whiteside, R. A.; Hout, R. F.; Hehre, W. J. *Int. J. Quantum Chem.* **1981**, *15*, 269.
(26) Yamaguchi, Y.; Schaeffer, H. F. *J. Chem. Phys.* **1980**, *73*, 2310.